

8.5 VOLTAGE-CONTROLLED OSCILLATORS

Most oscillators must be tuned over a certain frequency range. We therefore wish to construct oscillators whose frequency can be varied electronically. “Voltage-controlled oscillators” (VCOs) are an example of such circuits.

Figure 8.24 conceptually shows the desired behavior of a VCO. The output frequency varies from ω_1 to ω_2 (the required tuning range) as the control voltage, V_{cont} , goes from V_1 to V_2 . The slope of the characteristic, K_{VCO} , is called the “gain” or “sensitivity” of the VCO and expressed in rad/Hz/V. We formulate this characteristic as

$$\omega_{out} = K_{VCO} V_{cont} + \omega_0, \quad (8.43)$$

where ω_0 denotes the intercept point on the vertical axis. As explained in Chapter 9, it is desirable that this characteristic be relatively linear, i.e., K_{VCO} not change significantly across the tuning range.

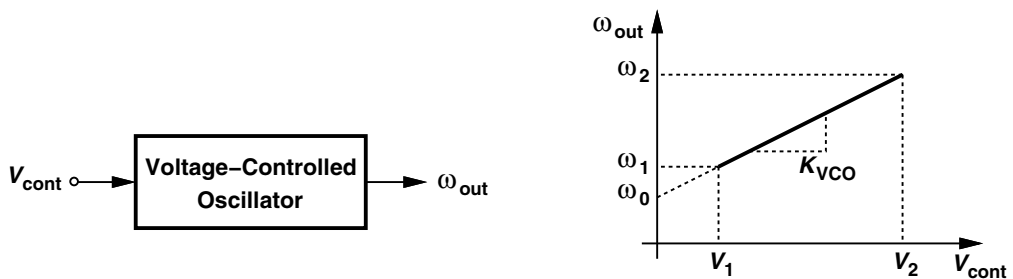


Figure 8.24 VCO characteristic.

Example 8.13

As explained in Example 8.12, the cross-coupled oscillator exhibits sensitivity to V_{DD} . Considering V_{DD} as the “control voltage,” determine the gain.

Solution:

We have

$$\omega_{osc} = \frac{1}{\sqrt{L_1(C_1 + C_{DB})}}, \quad (8.44)$$

where C_1 includes all circuit capacitances except C_{DB} . Thus,

$$K_{VCO} = \frac{\partial \omega_{out}}{\partial V_{DD}} \quad (8.45)$$

$$= \frac{\partial \omega_{osc}}{\partial C_{DB}} \cdot \frac{\partial C_{DB}}{\partial V_{DD}}. \quad (8.46)$$

The junction capacitance, C_{DB} , is approximated as

$$C_{DB} = \frac{C_{DB0}}{\left(1 + \frac{V_{DD}}{\phi_B}\right)^m}, \quad (8.47)$$

where ϕ_B denotes the junction’s built-in potential and m is around 0.3 to 0.4. It follows from Eqs. (8.46) and (8.47) that

$$K_{VCO} = \frac{-1}{2\sqrt{L_1}} \cdot \frac{1}{\sqrt{C_1 + C_{DB}(C_1 + C_{DB})}} \cdot \frac{-mC_{DB0}}{\phi_B \left(1 + \frac{V_{DD}}{\phi_B}\right)^{m+1}} \quad (8.48)$$

$$= \frac{C_{DB}}{C_1 + C_{DB}} \cdot \frac{m}{2\phi_B + 2V_{DD}} \omega_{osc}. \quad (8.49)$$

In order to vary the frequency of an LC oscillator, the resonance frequency of its tank(s) must be varied. Since it is difficult to vary the inductance electronically, we only vary the capacitance by means of a varactor. As explained in Chapter 7, MOS varactors are more commonly used than pn junctions, especially in low-voltage design. We thus construct our first VCO as shown in Fig. 8.25(a), where varactors M_{V1} and M_{V2} appear in *parallel* with the tanks (if V_{cont} is provided by an ideal voltage source). Note that the gates of the varactors are tied to the oscillator nodes and the source/drain/ n -well terminals to V_{cont} . This avoids loading X and Y with the capacitance between the n -well and the substrate.

Since the gates of M_{V1} and M_{V2} reside at an average level equal to V_{DD} , their gate-source voltage remains positive and their capacitance *decreases* as V_{cont} goes from zero to V_{DD} [Fig. 8.25(b)]. This behavior persists even in the presence of large voltage swings at X and Y and hence across M_{V1} and M_{V2} . The key point here is that the *average* voltage

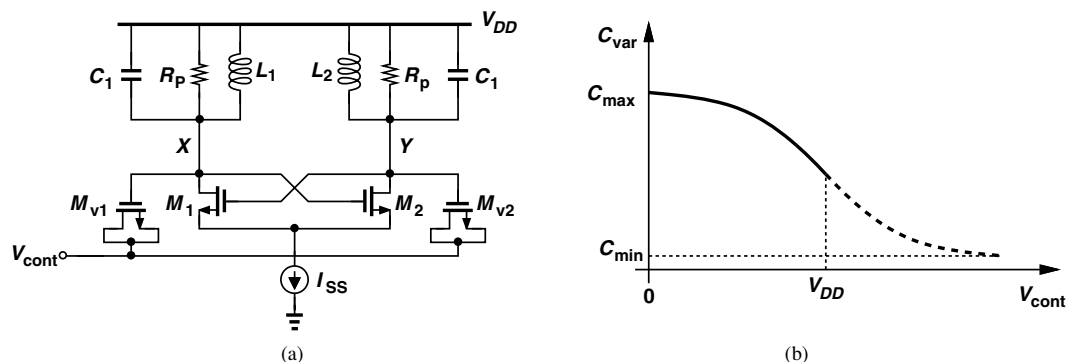


Figure 8.25 (a) VCO using MOS varactors, (b) range of varactor capacitance used in (a).

across each varactor varies from V_{DD} to zero as V_{cont} goes from zero to V_{DD} , thus creating a monotonic decrease in their capacitance. The oscillation frequency can thus be expressed as

$$\omega_{osc} = \frac{1}{\sqrt{L_1(C_1 + C_{var})}}, \quad (8.50)$$

where C_{var} denotes the average value of each varactor's capacitance.

The reader may wonder why capacitors C_1 have been included in the oscillator of Fig. 8.25(a). It appears that, without C_1 , the varactors can vary the frequency to a greater extent, thereby providing a wider tuning range. This is indeed true, and we rarely need to add a constant capacitance to the tank deliberately. In other words, C_1 simply models the inevitable capacitances appearing at X and Y : (1) C_{GS} , C_{GD} (with a Miller multiplication factor of two), and C_{DB} of M_1 and M_2 , (2) the parasitic capacitance of each inductor, and (3) the input capacitance of the next stage (e.g., a buffer, divider, or mixer). As mentioned in Chapter 4, the last component becomes particularly significant on the transmit side due to the “propagation” of the capacitance from the input of the PA to the input of the upconversion mixers.

The above VCO topology merits two remarks. First, the varactors are stressed for part of the period if V_{cont} is near ground and V_X (or V_Y) rises significantly above V_{DD} . Second, as depicted in Fig. 8.25(b), only about half of $C_{max} - C_{min}$ is utilized in the tuning. We address these issues later in this chapter.

As explained in Chapter 7, symmetric spiral inductors excited by differential waveforms exhibit a higher Q than their single-ended counterparts. For this reason, L_1 and L_2 in Fig. 8.25 are typically realized as a single symmetric structure. Figure 8.26 illustrates the idea and its circuit representation. The point of symmetry of the inductor (its “center tap”) is tied to V_{DD} . In some of our analyses, we omit the center tap connection for the sake of simplicity.

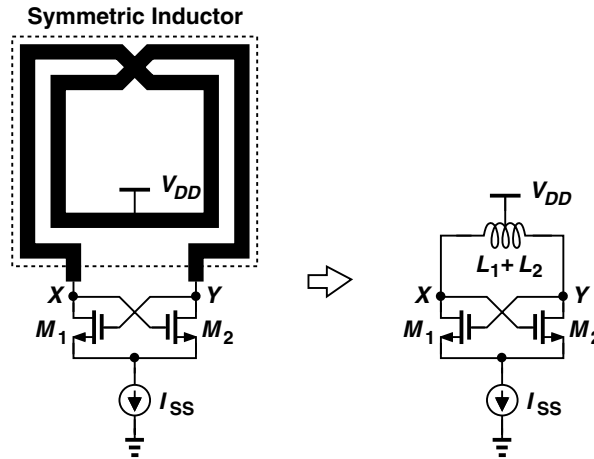


Figure 8.26 Oscillator using symmetric inductor.

Example 8.14

The symmetric inductor in Fig. 8.26 has a value of 2 nH and a Q of 10 at 10 GHz. What is the minimum required transconductance of M_1 and M_2 to guarantee startup?

Solution:

The parallel equivalent resistance of $L_1 + L_2 = 2$ nH is equal to $Q(L_1 + L_2)\omega = 1.26$ k Ω . From Eq. (8.40), we have

$$g_{m1,2} \geq (630 \Omega)^{-1}. \quad (8.51)$$

Alternatively, we can decompose the inductor into L_1 and L_2 and return to the circuit of Fig. 8.18(b). In this case, $R_p = QL_1\omega = QL_2\omega = 630 \Omega$, and $g_{m1,2}R_p \geq 1$. Thus, $g_{m1,2} \geq (630 \Omega)^{-1}$. The point here is that, for frequency and startup calculations, we can employ the one-port model with $L_1 + L_2$ as one inductor or the feedback model with L_1 and L_2 belonging to two stages.

The VCO of Fig. 8.25(a) provides an output CM level near V_{DD} , an advantage or disadvantage depending on the next stage (Section 8.9).

8.5.1 Tuning Range Limitations

While a robust, versatile topology, the cross-coupled VCO of Fig. 8.25(a) suffers from a narrow tuning range. As mentioned above, the three components comprising C_1 tend to limit the effect of the varactor capacitance variation. Since in (8.50), C_{var} tends to be a

small fraction of the total capacitance, we make a crude approximation, $C_{var} \ll C_1$, and rewrite (8.50) as

$$\omega_{osc} \approx \frac{1}{\sqrt{L_1 C_1}} \left(1 - \frac{C_{var}}{2C_1} \right). \quad (8.52)$$

If the varactor capacitance varies from C_{var1} to C_{var2} , then the tuning range is given by

$$\Delta\omega_{osc} \approx \frac{1}{\sqrt{L_1 C_1}} \frac{C_{var2} - C_{var1}}{2C_1}. \quad (8.53)$$

For example, if $C_{var2} - C_{var1} = 20\%C_1$, then the tuning range is about $\pm 5\%$ around the center frequency.

What limits the capacitance range of the varactor, $C_{var2} - C_{var1}$? We note from Chapter 7 that $C_{var2} - C_{var1}$ trades with the Q of the varactor: a longer channel reduces the relative contribution of the gate-drain and gate-source overlap capacitances, widening the range but lowering the Q . Thus, the tuning range trades with the overall tank Q (and hence with the phase noise).

Another limitation on $C_{var2} - C_{var1}$ arises from the available range for the control voltage of the oscillator, V_{cont} in Fig. 8.25(a). This voltage is generated by a “charge pump” (Chapter 9), which, as any other analog circuit, suffers from a limited output voltage range. For example, a charge pump running from a 1-V supply may not be able to generate an output below 0.1 V or above 0.9 V. The characteristic of Fig. 8.25(b) therefore reduces to that depicted in Fig. 8.27.

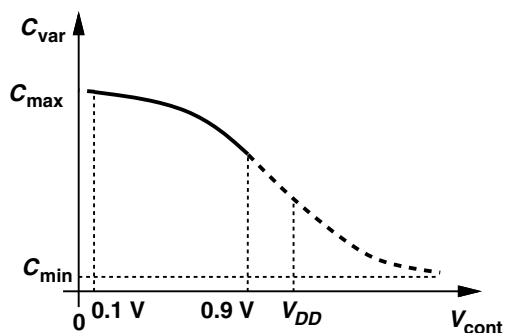


Figure 8.27 Varactor range used with input limited between 0.1 V and 0.9 V.

The foregoing tuning limitations prove serious in LC VCO design. We introduce in Section 8.6 a number of oscillator topologies that provide a wider tuning range—but at the cost of other aspects of the performance.

8.5.2 Effect of Varactor Q

As observed in the previous section, the varactor capacitance is but a small fraction of the total tank capacitance. We therefore surmise that the resistive loss of the varactor lowers the overall Q of the tank only to some extent. Let us begin with a fundamental observation.

Example 8.15

A lossy inductor and a lossy capacitor form a parallel tank. Determine the overall Q in terms of the quality factor of each.

Solution:

The loss of an inductor or a capacitor can be modeled by a parallel resistance (for a narrow frequency range). We therefore construct the tank as shown in Fig. 8.28, where the

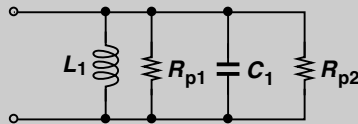


Figure 8.28 Tank consisting of lossy inductor and lossy capacitor.

inductor and capacitor Q 's are respectively given by

$$Q_L = \frac{R_{p1}}{L_1 \omega} \quad (8.54)$$

$$Q_C = R_{p2} C_1 \omega. \quad (8.55)$$

Note that, in the vicinity of resonance, $L_1 \omega = (C_1 \omega)^{-1}$. Merging R_{p1} and R_{p2} yields the overall Q :

$$Q_{tot} = \frac{R_{p1} R_{p2}}{R_{p1} + R_{p2}} \cdot \frac{1}{L_1 \omega} \quad (8.56)$$

$$= \frac{1}{\frac{L_1 \omega}{R_{p1}} + \frac{L_1 \omega}{R_{p2}}} \quad (8.57)$$

$$= \frac{1}{\frac{L_1 \omega}{R_{p1}} + \frac{1}{R_{p2} C_1 \omega}}. \quad (8.58)$$

It follows that

$$\frac{1}{Q_{tot}} = \frac{1}{Q_L} + \frac{1}{Q_C}. \quad (8.59)$$